Chemical Engineering Journal 111 (2005) 135–144

Chemical Engineering Journal

www.elsevier.com/locate/cej

Further development of software for the design and simulation of industrial thickeners

R. Burgos, F. Concha *

Departamento de Ingeniería Metalúrgica, Universidad de Concepción, Casilla 53-C, Concepción, Chile

Abstract

The authors presented at the Engineering Foundation Conference on Solid–Liquid Separation Systems III-2001 in Davos, software for the simulation of batch and continuous thickeners. The steady state of a continuous cylindrical thickener was simulated using the solid feed flux density function, the critical concentration, the solid effective stress and the required underflow concentration as input, in addition to the solid and fluid material densities. If the thickener area is known, the capacity and the concentration profile in the equipment are predicted. On the other hand, if the capacity is known, the required settling area and the resulting concentration profiles are predicted.

In the present work, the software is extended to thickeners having conical bottoms. As model functions, two choices are possible, a solid flux density function for the whole range of solid concentrations or a solid flux density function for concentrations less than the critical and a sediment permeability and an effective solid stress for concentration above the critical. The following outputs can be chosen, the unit area, the cross-sectional area for a given capacity and height of sediment, the plot of sediment height versus thickener area for a given capacity, the plot of sediment height versus capacity for a given thickener area and the concentration profiles and mass balances for any of these cases.

Keywords: Tailings; Dewatering; Thickening; Modeling; Simulation

1. Introduction

1.1. Theory and practice

All what is presently known on industrial thickeners was discovered during the twentieth century: from the concept and construction of the first industrial thickener in 1905 to the present mathematical analysis of the modern thickening theories [1,2].

The invention of the Dorr thickener [3,4] made the continuous dewatering of dilute pulps possible. Mishler [5,6] was the first to show by experiment that the rate of settling of slimes is different for dilute than for concentrated suspensions. While the settling speed of dilute slimes is usually independent of the depth of the settling column, for thick slimes sedimentation rate increases with the depth of the settling column. Two of the most important features in the operation of a thickener were expressed for the first time in 1954 by Comings et al. [7]. In the first place, they established that the concentration in the settling zone is nearly constant for a thickener at steady state, and that its concentration depends on the rate at which the solid is fed to the thickener. It was verified that in most cases the feed *is diluted* to an unknown concentration on entering the thickener. The second finding was that, for the same feed rate, increasing or decreasing the sediment depth could adjust the underflow concentration.

In 1952, Kynch [8] presented in his paper "*A theory of sedimentation*", a kinematical theory based on the propagation of concentration waves in the suspension. Experience by several authors, among them Shannon et al. [9], demonstrated that, Kynch's theory is suitable for suspension of equally sized, rigid particles known as *ideal suspensions*. Unfortunately, Kynch's theory cannot be regarded as appropriate for flocculent suspensions since it ignores the compressibility of the sediment formed at the bottom of the thickener [10–16].

Based on the Theory of Mixtures, the phenomenological theory of sedimentation extended Kynch's theory to compressible pulps [17–19]. This theory shows that Kynch's theory of ideal suspensions is valid for all types of suspensions, compressible or not, for regions where the concentration is

* Corresponding author. Tel.: +56 41 236810; fax: +56 41 230759.
E-mail address: fconcha@udec.cl (F. Concha).

1385-8947/$ – see front matter © 2005 Elsevier B.V. All rights reserved.
doi:10.1016/j.cej.2005.02.012

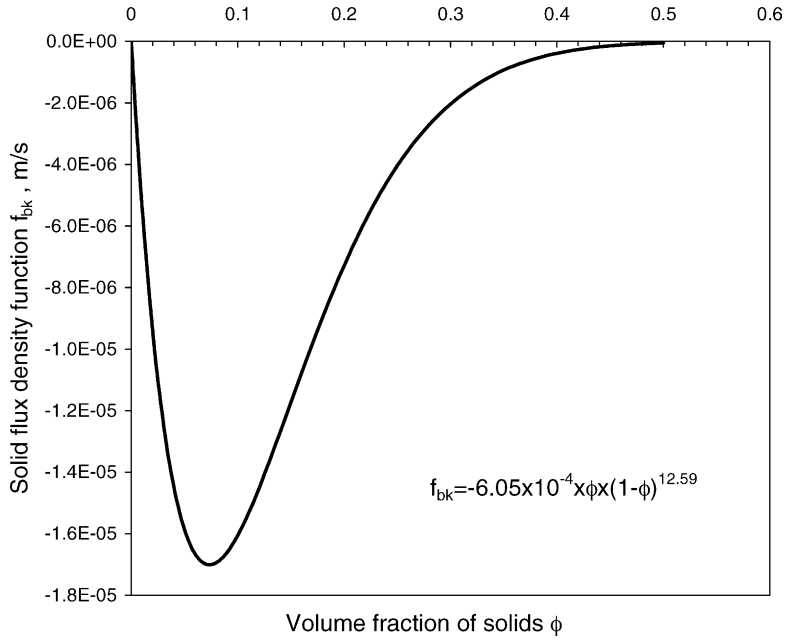

Fig. 1. Constitutive function for the solid flux density $f_{bk}(\varphi)$, [24].

small, less than the critical concentration, but a term related to the compressibility of the sediment exists for higher concentrations. At the end of the seventies and during the eighties, several papers [1] show that the phenomenological model, based on the mixture theory, was well accepted by the international scientific community.

1.2. Thickener design

Arguing that the solid handling capacity (today called solid flux-density) has a maximum value at a certain concentration between the feed and the discharge concentrations in the thickener, Coe and Clevenger [20], developed an equa-

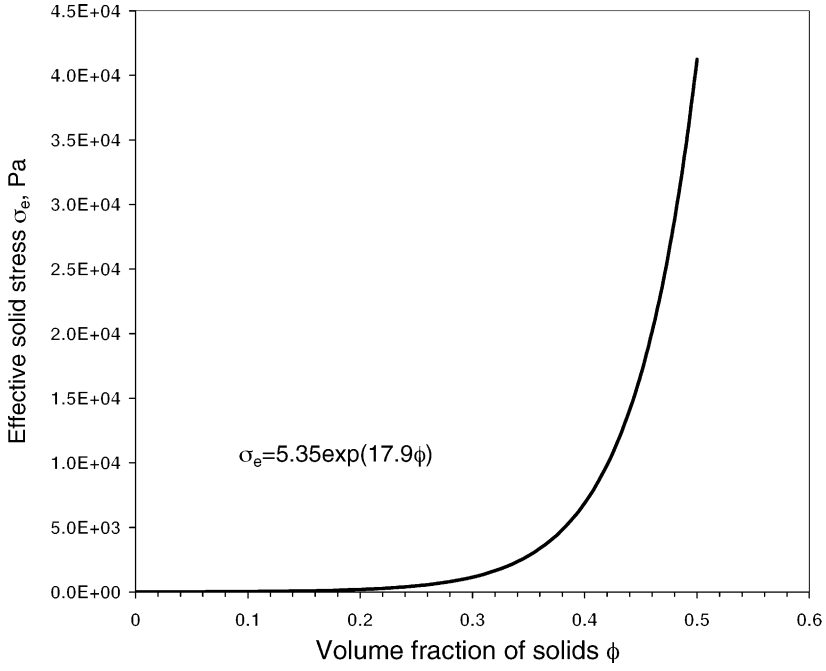

Fig. 2. Constitutive function for the effective solid stress $\sigma_e(\varphi)$, [24].

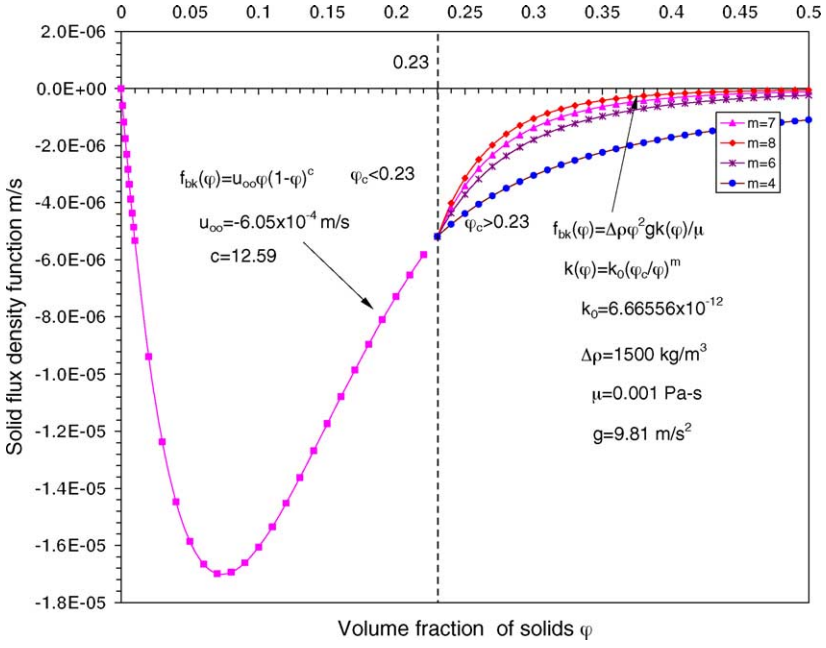

Fig. 3. Constitutive function for a solid flux density $f_{bk}(\varphi)$ with several m values for the permeability parameter.

tion to calculate the unit area:

$$UA_0 = \max_{\mathcal{D}_F > \mathcal{D}_k > \mathcal{D}_U} \frac{\mathcal{D}_k - \mathcal{D}_U}{\rho_f v_s(\mathcal{D}_k)} \quad (1)$$

where UA_0 is the unit area (thickener area/daily capacity), $\mathcal{D}$ the pulp dilution (mass of water/mass of solid), ρ_s the solid mass density, $v_s(\mathcal{D}_k)$ the initial settling velocity of a suspension of dilution $\mathcal{D}_k$ and the subscript F and U denote feed and underflow, respectively. The method requires performing several laboratory experiments to calculate the initial settling velocities of the solid from suspensions with dilutions from the feed to the underflow.

Since the volume fraction of solids is related to the dilution through $\mathcal{D} = \rho_f(1-\varphi)/\rho_p\varphi$, Eq. (1) may be written in the form

$$UA_0 = \max_{\varphi_F < \varphi < \varphi_D} \frac{1}{\rho_s \varphi_k v_s(\varphi_k)} \left(\frac{\varphi_k}{\varphi_U} - 1 \right). \quad (2)$$

Coe and Clevenger's design procedure was the only quantitative knowledge in sedimentation accomplished during the first half of the 20th century [20].

Based on Kynch's theory of sedimentation several authors [10,11,13,21,22] devised methods of thickener design. They affirmed that one settling plot had all the information needed to design a thickener and therefore only one laboratory sedimentation experiment was necessary. Since in this settling

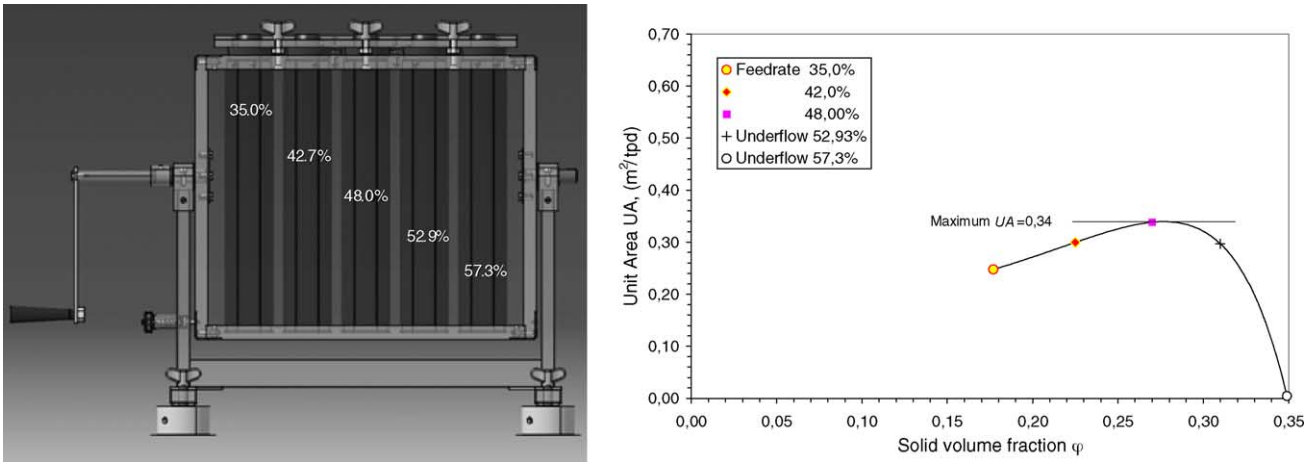

Fig. 4. Settling experiments with copper tailings from the feed to the underflow concentrations, according to Coe and Clevenger's method [20]. On the left, a sedimentation rack permits to perform the settling experiments, for suspensions at five different concentrations, in the same conditions of initial agitation. At the right, a plot shows the calculated unit areas from the experiments at different concentrations.

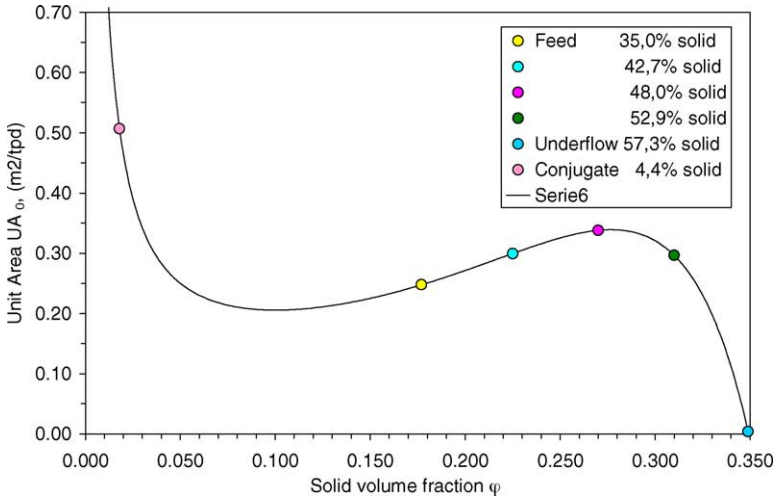

Fig. 5. Settling experiment with copper tailings from the conjugate to the underflow concentrations, according to the phenomenological theory of sedimentation.

plot, the slope of the water–suspension interface gave the settling velocity of the suspension, the slope at different times should represent the settling velocity at different concentrations. For more details, see [23].

A suspension is said to be in *hindered settling* when the particles (flocs) fall independently one from another and it is in *consolidation* when the particles (flocs) touch each other permanently during sedimentation. We assume that the process changes from settling to consolidation (or compression) at a critical concentration denoted by φ_c. The phenomenological theory [18,19] characterizes the sedimentation by the volume fraction of solid $\varphi(z, t)$, the Kynch solid flux density function $f_{bk}(\varphi)$, the volume average velocity $q(t)$ and by the solid effective stress $\sigma_e(\varphi)$. These four variables must obey the field equation (3), and constitutive equations such as (4) and (5).

$$\frac{\partial \varphi}{\partial t} + \frac{\partial}{\partial z}(q(t)\varphi + f_{bk}(\varphi)) = -\frac{\partial}{\partial z}\left(f_{bk}(\varphi)\frac{\sigma_e'(\varphi)}{\Delta\rho\varphi g}\frac{\partial \varphi}{\partial z}\right), \quad 0 \le z \le L, t > 0, \tag{3}$$

$$f_{bk}(\varphi) = u_\infty \varphi\left(1 - \frac{\varphi}{\varphi_{max}}\right)^c, \quad q(t) \le 0 \tag{4}$$

$$\sigma_e(\varphi) = \begin{cases} 0 & \text{for } \varphi \le \varphi_c, \\ \alpha \exp(\beta\varphi) \quad \text{or} \quad \sigma_0\left\{\left(\frac{\varphi}{\varphi_c}\right)^n - 1\right\} & \text{for } \varphi > \varphi_c, \end{cases} \tag{5}$$

The special characteristics of each material is described by the constitutive functions $f_{bk}(\varphi)$ and $\sigma_e(\varphi)$, where $f_{bk}(\varphi) \le 0$, $f_{bk}(0) = f_{bk}(1) = 0$ for $0 \le \varphi \le 1$. Here α, β, σ_0, n, φ_{max} and c are positive numbers, while $u_\infty < 0$. Typical constitutive functions are shown in Figs. 1 and 2. Eq. (3) is of first-order hyperbolic type for $\varphi \le \varphi_c$ or $\varphi > 1$ and of second-order parabolic type for $\varphi_c < \varphi < 1$.

Coe and Clevenger's method [20] and those based on Kynch's theory, characterize the pulp with only one parameter, the initial sedimentation velocity determined with laboratory experiments. The design methods based on the phenomenological theory use three properties to characterize the pulp, the initial settling velocity, the critical concentration and the compressibility of the sediment.

Fig. 6. SimEsp Software.

1.3. Thickeners with varying cross-section

All industrial thickeners have three sections with different areas. In the first place, the feedwell diminishes the area for the flow of recovered water and the bottom of the tank is

usually of conical shape to aid in the underflow discharge. The ideal continuous thickener (ICT), [25–27] used for modeling a real thickener ignores these facts and assumes a constant cross-section for the equipment. Bürger et al. [28] showed that a thickener with varying cross-section could be represented by the following field balance equation instead of (3):

$$\frac{\partial\varphi}{\partial t}+\frac{1}{S(z)}\frac{\partial}{\partial z}(-Q_{\mathrm{U}}(t)\varphi+S(z)f_{\mathrm{bk}}(\varphi)) = \frac{1}{S(z)}\frac{\partial}{\partial z}\left(S(z)\frac{-f_{\mathrm{bk}}(\varphi)\sigma_{\mathrm{e}}'(\varphi)}{\Delta\rho\varphi g}\frac{\partial\varphi}{\partial z}\right),$$
$$\text{for } 0\le z\le L, t>0 \tag{6}$$

where φ is the pulp concentration, $S(z)$ the variable cross-sectional area of the thickener, Q_{U} the volume underflow rate, f_{bk} the batch solid flux density function, σ_{e} the solid effective stress, $\Delta\rho=\rho_{\mathrm{s}}-\rho_{\mathrm{f}}$ the solid–liquid density difference and g is the acceleration of gravity constant.

Equation (6) is a degenerate parabolic partial differential equation, which transforms to a hyperbolic equation, representing the sedimentation of an ideal suspension, when the concentration is less or equal to the critical, $\varphi\le\varphi_{\mathrm{c}}$:

$$\frac{\partial\varphi}{\partial t}+\frac{1}{S(z)}\frac{\partial}{\partial z}(-Q_{\mathrm{U}}(t)\varphi+S(z)f_{\mathrm{bk}}(\varphi))=0,$$
$$\text{for } 0\le z\le L, t>0 \tag{7}$$

1.4. Steady state

At steady state a macroscopic balance yields

$$Q_{\mathrm{F}}\varphi_{\mathrm{F}}=Q_{\mathrm{U}}\varphi_{\mathrm{U}} \tag{8}$$

$L,\varphi_{\mathrm{L}},z_{\mathrm{c}}/L,\varphi_{\mathrm{F}},\varphi_{\mathrm{D}},\varphi_{\mathrm{c}},\rho_{\mathrm{s}},\rho_{f},f_{bk}(\varphi),\sigma_{e}(\varphi)$

↓

Determine $AU(\varphi,\varphi_D)=\dfrac{1}{\rho_s f_{bk}(\varphi)}\left(\dfrac{\varphi}{\varphi_D}-1\right)$

Find maximum $AU_0(\varphi_L\le\varphi\le\varphi_D)$.

Calculate $S=UA_0\times F$.

Calculate D.

Integrate the concentration profile from

$$\frac{\mathrm{d}z}{\mathrm{d}\varphi}=-\frac{\sigma_e'(\varphi)f_{bk}(\varphi)}{\Delta\rho\varphi g}\left(\frac{Q_D}{S(z)}(\varphi-\varphi_D)+f_{bk}(\varphi)\right)$$

with $\varphi(0)=\varphi_D$.

Determine z_c. If $z_c\neq 0.20L$, iterate changing D to meet $z_c/L\approx 0.20$.

Increase D to the next integer.

(Determine D as a function of z/L.)

Make a new calculation.

Find the result: UA,S,D,φ_L,q,f_F.

(Determine F as a function of z/L).

Fig. 7. Algorithm used by SimEsp.

where Q_{F} and Q_{U} are the feed and underflow pulp volume flow rate. With a similar analysis than in Garrido et al. [29,30], the basic unit area UA_0, defined in this case as the maximum of the cylindrical section of the thickener, is given by:

$$\mathrm{UA}_0=\max_{\varphi_{\mathrm{L}}\le\varphi\le\varphi_{\mathrm{U}}}\left\{\frac{1}{\rho_{\mathrm{s}}f_{\mathrm{bk}}(\varphi)}\left(\frac{\varphi}{\varphi_{\mathrm{U}}}-1\right)\right\},$$
$$\varphi_{\mathrm{L}}\le\varphi\le\varphi_{\mathrm{U}} \tag{9}$$

And the concentration profile by [28]:

$$\frac{\mathrm{d}\varphi}{\mathrm{d}z}=\frac{\Delta\rho\varphi g}{f_{\mathrm{bk}}(\varphi)\sigma_{\mathrm{e}}'(\varphi)}\left(-\frac{Q_{\mathrm{U}}}{S(z)}(\varphi(z)-\varphi_D)+f_{\mathrm{bk}}(\varphi(z))\right),$$
$$0\le z\le z_{\mathrm{c}} \tag{10}$$

$$Q_{\mathrm{U}}\varphi(z)+S(z)f_{\mathrm{bk}}(\varphi(z))=Q_{\mathrm{F}}\varphi_{\mathrm{F}},\quad \text{for } z>z_{\mathrm{c}} \tag{11}$$

$$\varphi=\varphi_D\quad\text{for } z=0 \tag{12}$$

Equation (10) can be solved with the boundary condition (12) to obtain the concentration profile in the thickener.

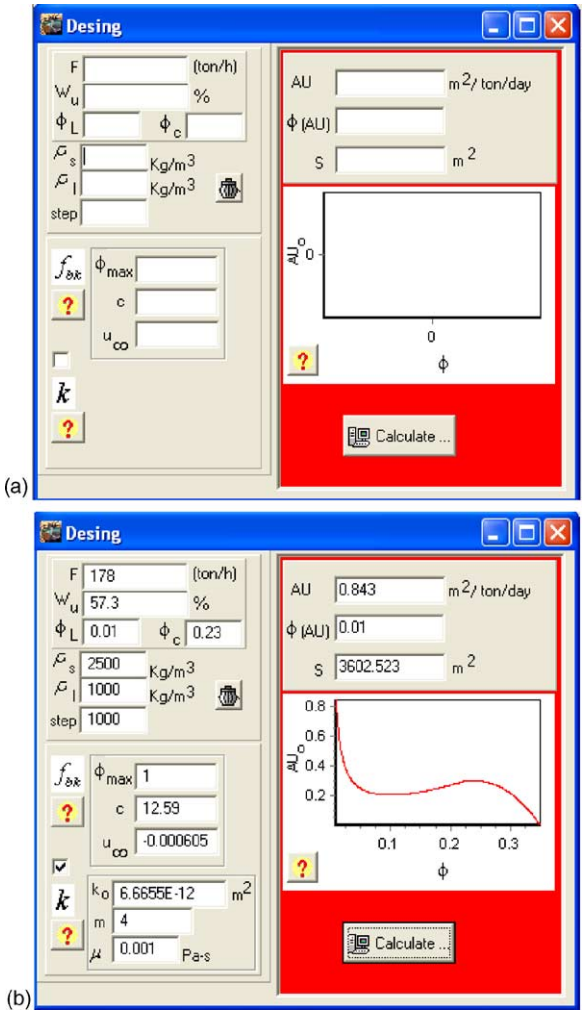

Fig. 8. (a and b) Design modules.

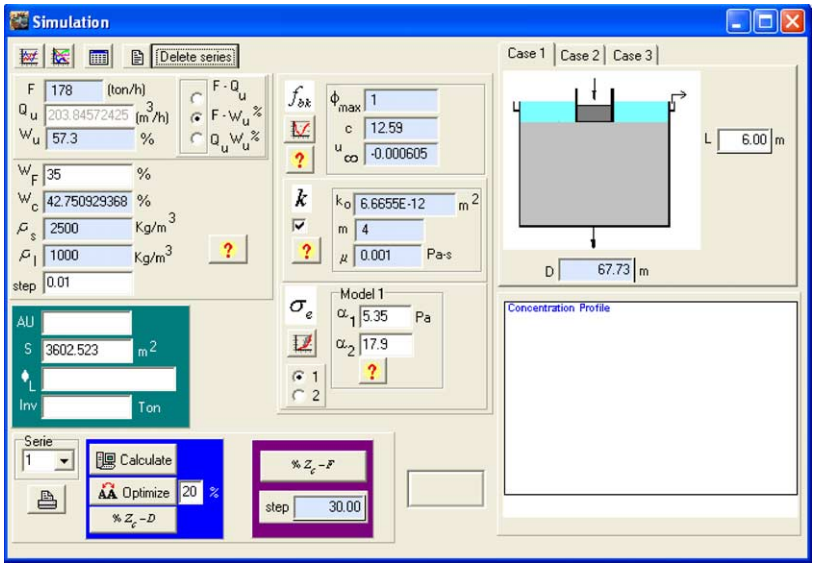

Fig. 9. Simulation module.

1.5. Thickening parameters

The batch solid flux density function may be obtained from settling experiments alone or from settling experiments for concentrations less than the critical and from sediment permeability tests for values of concentration greater than the critical. The parameters $f_{bk}(\varphi)$ and the solid effective stress $\sigma_e(\varphi)$ may be expressed alternatively with the following constitutive equations:

$$f_{bk}(\varphi) = \begin{cases} u_\infty \varphi \left(1 - \dfrac{\varphi}{\varphi_{max}}\right)^c, & \text{for } \varphi_L \le \varphi \le \varphi_m, \text{ or} \\ u_\infty \varphi \left(1 - \dfrac{\varphi}{\varphi_{max}}\right)^c, & \text{for } \varphi \ge \varphi_c, \text{ and} \\ \dfrac{\Delta\rho}{\mu}\varphi^2 g k(\varphi), & \text{for } \varphi \ge \varphi_c \end{cases} \quad (13)$$

$$\sigma_e(\varphi) = \begin{cases} 0, & \text{for } \varphi \le \varphi_c, \\ \alpha \exp(\beta\varphi), & \text{for } \varphi > \varphi_c, \text{ or} \\ \sigma_0 \left\{ \left(\dfrac{\varphi}{\varphi_c}\right)^n - 1 \right\}, & \text{for } \varphi > \varphi_c \end{cases} \quad (14)$$

where the permeability of the sediment may be modeled in the form [31]: $k(\varphi) = (\Delta\rho/\mu)\varphi^2 g k_0 (\varphi_c/\varphi)^m$. Fig. 3 shows the solid flux density function using the permeability with different values of the parameter m.

In conclusion, the basic unit area derived from the phenomenological theory, equation (9), has the same form as that proposed by Coe and Clevenger in 1916 [20], equation (2), except for the fact that the range of validity of the equation is from the conjugate concentration φ_L, instead of the feed concentration φ_F, to the underflow concentration φ_U. This small detail is of the greatest importance in most cases.

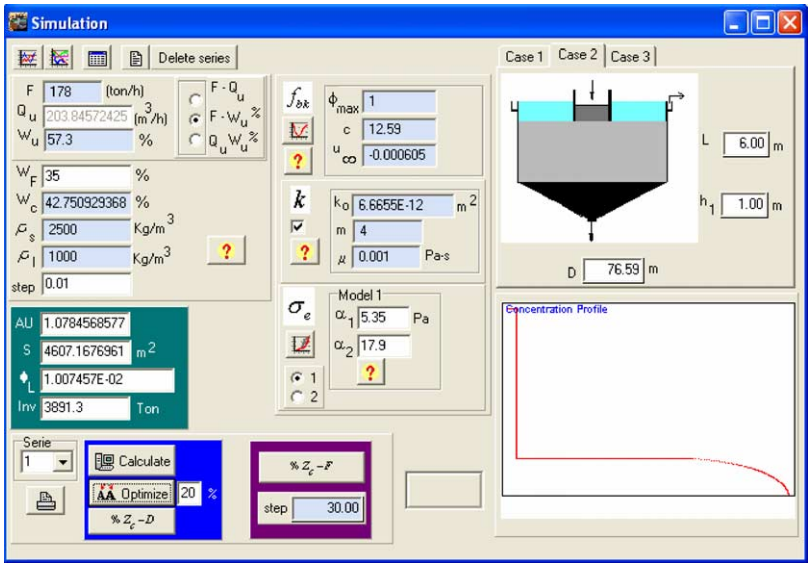

Fig. 10. *Optimization* choice in the Simulator Module.

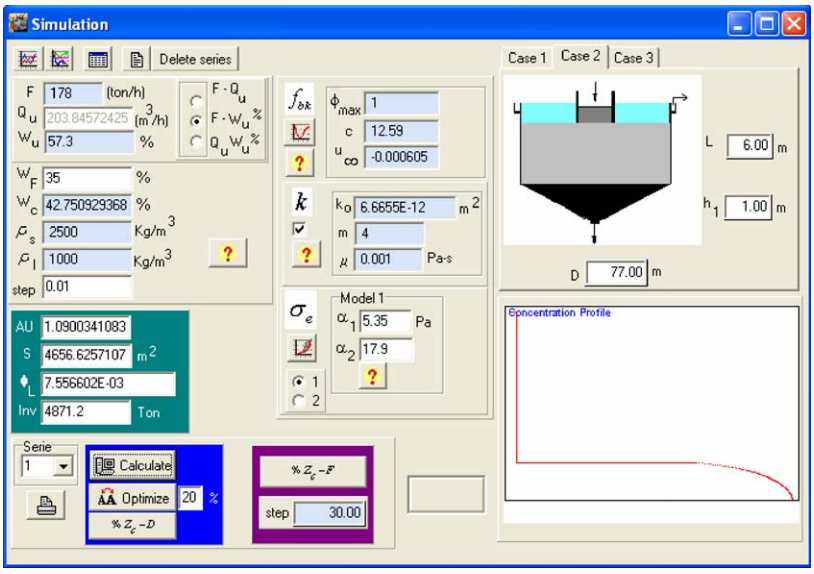

Fig. 11. *Calculate* choice of the Simulation Module.

Example 1. Take, for example, experiments made to design a continuous thickener for a feed rate of 178 t/h with the following concentrations of a copper tailing: 35.0, 42.0, 48.0, 52.9 and 57.3% solid by weight, where the first and the last concentrations correspond to the feed and the desired underflow.

Fig. 4 shows the unit area obtained for each of the concentrations φ. According to Coe and Clevenger, and the maximum of them is, $UA_0 = 0.34\,m^2/(t\,d)$.

But a flat bottom thickener treating a copper tailing at a feed rate of $F = 178$ t/h, has a conjugate concentration of $\varphi_L = 0.018$ [29] and, therefore, the range of concentrations from the conjugate concentration to the feed concentration $\varphi_F = 0.177$ should also be considered. One more experimental test at concentration $\varphi_L = 0.01$ yields the following new result $UA_0 = 0.52\,m^2/(t\,d)$ (see Fig. 5). Figs. 4 and 5 show that Coe and Clevenger's method [20] gives, in this case, an error of 32% in basic the unit area.

The problem to calculate the maximum of $UA_0(\varphi, \varphi_D)$ with $\varphi_L \le \varphi \le \varphi_D$, is that the conjugate concentration φ_L is unknown until the value of the thickener area S is calculated, which is the result we are seeking for. Therefore, the problem is undetermined and, to solve it, a value of φ_L must be assumed, for example $\varphi_L \approx 0.01$. This problem may be solved with the software *SimEsp* (Fig. 6).

In designing a thickener with *SimEsp*, the desired feed flow rate F (tph) and underflow concentration φ_D, together with the thickening parameters $f_{bk}(\varphi)$ (m/s), φ_c and $\sigma_e(\varphi)$ (Pa) and the solid and liquid densities ρ_s and ρ_f, (kg/m^3) must be known. With these values, the function $UA_0\ (\varphi, \varphi_D)$ can be calculated for any value of φ.

The algorithm used can be seen in the following Fig. 7.

Example 2. Consider the design of an industrial thickener for a feed rate of 178 tph, with an underflow concentration of 57.3% of solid by weight of a copper tailing with the following properties:

Solid density	$\rho_s = 2500$ kg/m^3
Liquid density	$\rho_f = 1000$ kg/m^3
Feed concentration	$w_F = 35\%$ by weight
Critical concentration	$w_c = 42.7$ % by weight
Settling parameters	$u_\infty = -0.000605$ m/s, $c = 12.59$, $\varphi_{max} = 1$
Permeability parameters	$k_0 = 6.67 \times 10^{-12}$, $m = 4$
Fluid viscosity	$\mu = 0.001$ Pa s
Compression parameters	$\alpha_1 = 5.35$ Pa, $\alpha_2 = 17.9$
Thickener height	$L = 6$ m, height of conical bottom $h_1 = 1$ m
Sediment height	$z_c = 0.20L$

Open SimEsp and choose the *Design Module* (Fig. 8).

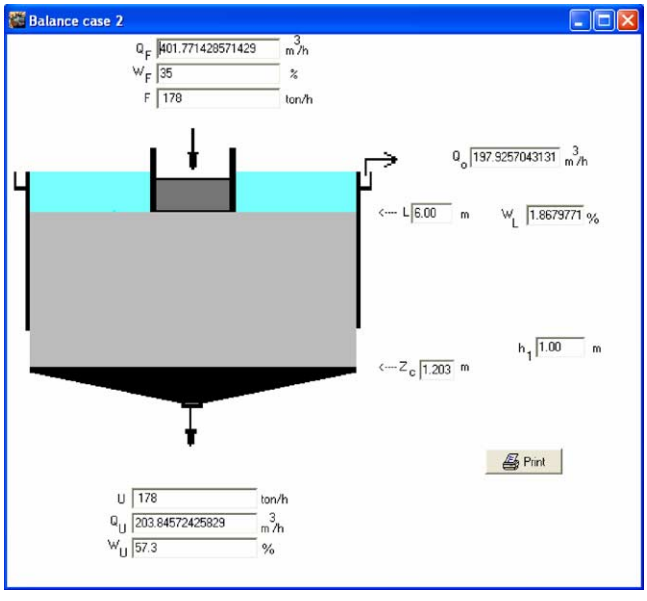

Fig. 12. Mass balance in the thickener.

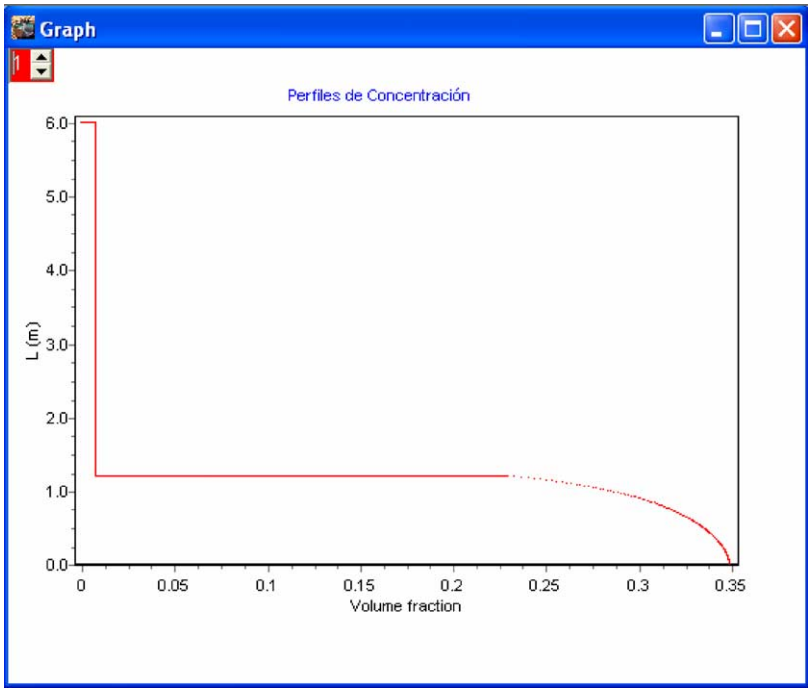

Fig. 13. Concentration profile in the thickener.

Fill the input data on the *Design Module* (Fig. 8a). By saving this information, future calculations may be made. Click the "Calculate" button to obtain the UA(φ) curve.

The curve representing the unit area function UA_0 appears and the values of $UA = \max_{\varphi_L \le \varphi \le \varphi_U} UA_0(\varphi, \varphi_U)$ and the concentration at which it occurs (Fig. 8b). The cross-sectional area needed by the thickener to treat the required tonnage is then calculated. The maximum unit area, for $\varphi_L = 0.01$, is $UA_0 = 0.843$ (m^2/tpd) at $\varphi = 0.01$.

With this result, run the *Simulation Module* (Fig. 9) to obtain the next figure.

Choose "Case 2" for a conical bottom thickener. Add the compression parameter information: α_1, α_2, or σ_0 and n and the desired thickener height $L = 6$ m and coni-

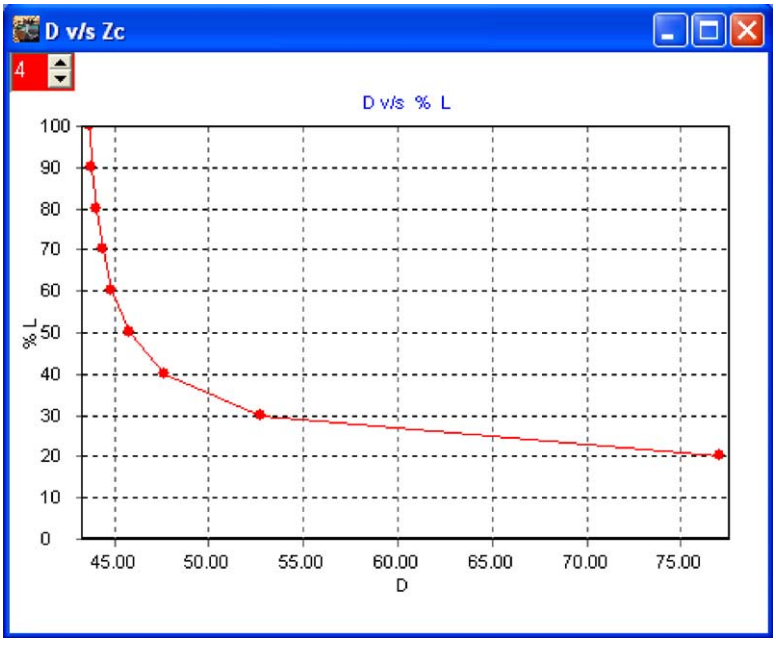

Fig. 14. Sediment height vs. diameter of thickener.

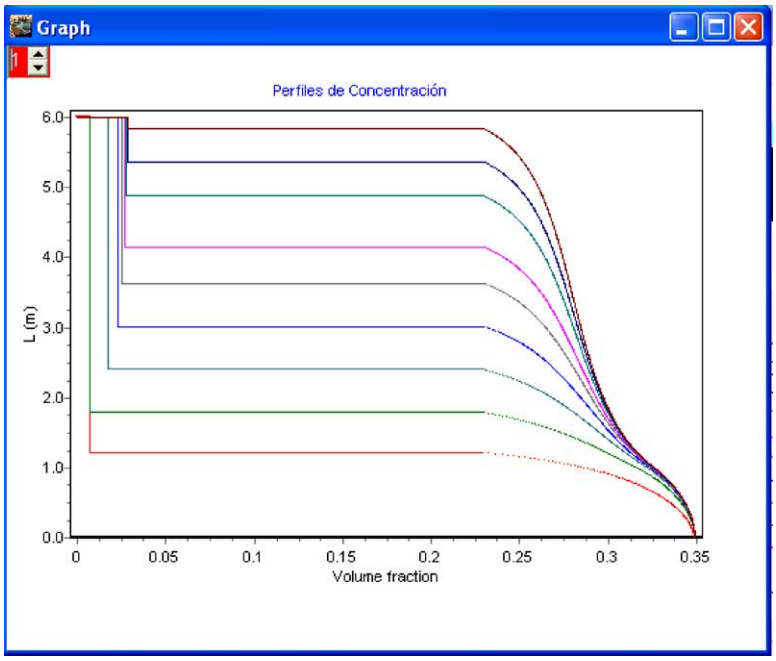

Fig. 15. Capacity of the designed thickener. The double curvature in the profiles is due to the conical bottom.

cal section height $h_1 = 1.0$ m; the desired sediment height 20% of L, and run the "Optimization" button. The simulator iterates until the desired height of sediment is obtained. The result is a thickener with diameter $D = 76.60$ m (Fig. 10).

Set the thickener diameter to the next integer, "$D = 77$ m", or to any other desired size, and choose the "Calculate" button of the Simulator and find the final result (Fig. 11).

The final results of the design procedure are a unit area of UA = 1.09 m^2/tpd, a thickener diameter of $D = 77$ m and a conjugate concentration of $\varphi_L = 7.56 \times 10^3$. A schematic version of the thickener with the mass balance and the concentration profile is shown in Figs. 12 and 13.

The thickener diameter $D = 77$ m, obtained in the previous example, is valid if the sediment is allowed to grow to 20% of the thickener height. The button "%$z_c - D$" allows to obtain designs with thickener diameters for any other value of the sediment height from 10 to 90%L with 10% increments. Fig. 14 shows this relationship.

Another possibility is to design the thickener for 20%L and to calculate the thickener capacity allowing other heights for the sediment from $z_c = 20$ to 100%. For this calculation, use the button "%$z_c - F$" (Figs. 15 and 16).

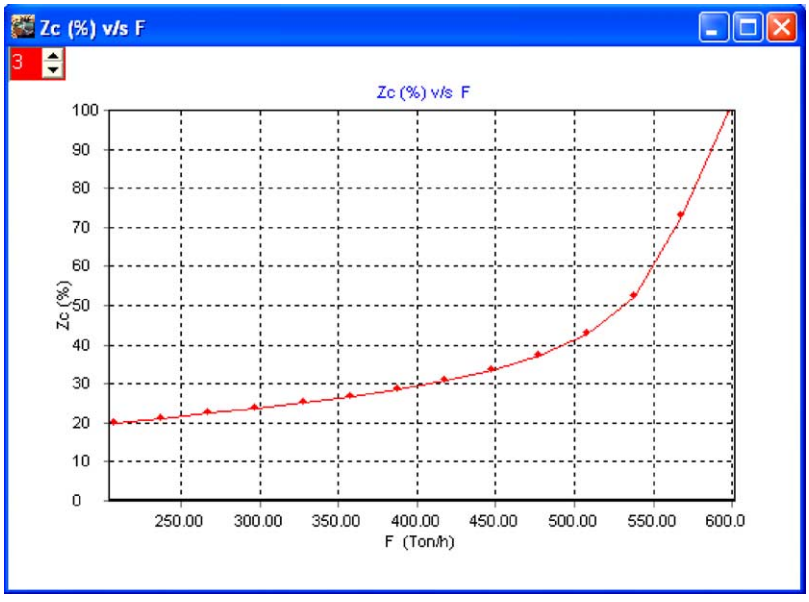

Fig. 16. Sediment height Vs. capacity for the designed thickener.

2. Conclusions

In our previous papers [29,30], we presented an algorithm for the simulation of batch and continuous thickening. In this work, we extend that work in several ways.

The first part of the design procedure, *Design Module*, makes use of the solution to the phenomenological model at steady state. The result is an equation similar to that of Coe and Clevenger [20] that seeks for the maximum unit area UA_0 between the conjugate concentration φ_L and the underflow concentration φ_D. An addition to the previous algorithm is the possibility to use permeability data for the flow of water through the sediment.

Next, the *Simulation Module* seeks for the thickener area S that gives a prescribed sediment height, for example, 20% of the total active thickener height L. The thickener diameter, in meters, is then approximated to the next integer. The results may be given in several numerical forms or in graphs indicating diameter, capacity and concentration profiles.

Additional graphs may be called to show the constitutive equations for $f_{bk}(\varphi)$ and $\sigma_e(\varphi)$.

In most practical problems, as those shown in this paper, the requirement for the sediment height to be $z_c/L = 0.20$, with the conical sections height being $h/L = 0.17$, leaves always the sediment above the height of the conical section. In these cases, the concentration in the settling zone is constant, $\varphi(z) = \varphi_L$, for $z > z_c$. Obviously, this is not the case in general. When the height z_c is smaller than the height of the conical section, the conjugate concentration φ_L is not constant, but varies with height. Moreover, there might be a continuous transition between the sediment level and the hindered settling zone (see for example [28]).

Acknowledgments

We acknowledge support by Fondecyt through project no. 1040597 and by the Mineral Technology Center Cettem Ltd.

References

[1] F. Concha, R. Bürger, A century of research in sedimentation and thickening, KONA, Powder Part. 20 (2002) 38–70.
[2] F. Concha, R. Bürger, Thickening in the 20th century: a historical perspective, Miner. Metall. Process. 20 (2003) 57–67.
[3] J.V.N. Dorr, The use of hydrometallurgical apparatus in chemical engineering, J. Ind. Eng. Chem. 7 (1915) 119–130.
[4] J.V.N. Dorr, Cynidation and Concentration of Gold and Silver Ores, McGraw-Hill Book Co. Inc., New York, 1936.
[5] R.T. Mishler, Settling slimes at the Tigre Mill, Eng. Min. J. 94 (1912) 643–646.
[6] R.T. Mishler, Methods for Determining the Capacities of Slime-Thickening Tanks, St. Louis Meeting, September, 1917, pp. 102–125.
[7] E.W. Comings, C.E. Pruiss, C. De Bord, Continuous settling and thickening, Ind. Eng. Chem. Des. Process. Dev. 46 (1954) 1164–1172.
[8] G.J. Kynch, Theory of sedimentation, Trans. Faraday Soc. 48 (1952) 166–176.
[9] P.T. Shannon, E.P. Stroupe, E.M. Tory, Batch and continuous thickening, Ind. Eng. Chem. Fund. 2 (1963) 203–211.
[10] N. Yoshioka, Y. Hotta, S. Tanaka, S. Naito, S. Tsugami, Continuous thickening of homogeneous flocculated slurries, Chem. Eng. Jpn. 21 (1957) 66–75.
[11] N.J. Hassett, Design and operation of continuous thickeners, Ind. Chem. 34 (1958) 116–120, 69–172, 489–494.
[12] N.J. Hassett, Theories of the operation of continuous thickeners, Ind. Chem. (January) (1961) 25–28.
[13] N.J. Hassett, Mechanism of thickening and thickener design, Trans. Inst. Min. Met. 74 (1964) 627–656.
[14] N.J. Hassett, Thickening in theory and practice, Min. Sci. Eng. 1 (1968) 24–40.
[15] K.J. Scott, Theory of thickening: Factors affecting settling rate of solids in flocculated pulps, Trans. Inst. Min. Met. Lond. 77 (1968) C85–C97.
[16] K.J. Scott, Thickening of calcium carbonate slimes, Ind. Eng. Chem. Fund. 7 (1986) 484.
[17] R. Bürger, F. Concha, Mathematical model and numerical simulation of the settling of flocculated suspensions, Int. J. Multiphase Flow 24 (1998) 1005–1023.
[18] R. Bürger, M.C. Bustos, F. Concha, Settling velocities of particulate systems: 9. Phenomenological theory of sedimentation processes: numerical simulation of the transient behavior of flocculated suspensions in an ideal batch or continuous thickener, Int. J. Miner. Process. 55 (1999) 267–282.
[19] M.C. Bustos, F. Concha, R. Bürger, E.M. Tory, Sedimentation and Thickening: Phenomenological Foundation and Mathematical Theory, Kluwer Academic Publishers, Dodrecht, The Netherlands, 1999, p. 304.
[20] H.S. Coe, G.H. Clevenger, Methods for determining the capacities of slime settling tanks, Trans. AIME 55 (1916) 356–385.
[21] W.P. Talmage, E.B. Fitch, Determining thickener unit areas, Ind. Eng. Chem. Eng. Des. Dev. 47 (1) (1955) 38–41.
[22] J.H. Wilhelm, Y. Naide, Sizing and operating continuous thickeners, Min. Eng. 33 (1981) 1710–1718.
[23] F. Concha, A. Barrientos, A critical review of thickener design methods, KONA, Powder Part. 11 (1993) 79–104.
[24] Becker, R., Espesamiento continuo: diseño y simulación de espesadores, Engineering Thesis, University of Concepción, 1982.
[25] P.T. Shannon, E.M. Tory, The analysis of continuous thickening, SME Trans. 235 (1966) 375–382.
[26] M.C. Bustos, F. Concha, W. Wendland, Global weak solutions to the problem of continuous sedimentation of an ideal suspension, Math. Meth. Appl. Sci. 13 (1990) 1–22.
[27] F. Concha, M.C. Bustos, Settling velocities of particulate systems part 6, Kynch sedimentation processes: batch settling, Int. J. Miner. Process. 34 (1992) 33–51.
[28] R. Bürger, J.J.R. Damasceno, K.H. Karlsen, A mathematical model for batch and continuous thickening in vessels with varying cross-section, Int. J. Mine. Process. 73 (2004) 183–208.
[29] P. Garrido, R. Burgos, F. Concha, R. Bürger, Software for the design and simulation of gravity thickeners, Miner. Eng., Pergamon 16 (2003) 85–92.
[30] P. Garrido, R. Burgos, F. Concha, R. Bürger, Settling velocities of particulate systems 13. Software for the batch and continuous sedimentation of flocculated suspensions, Int. J. Miner. Process. 73 (2004) 131–144.
[31] R. Burger, F. Concha, F.M. Tiller, Applications of the phenomenological theory to several published experimental cases of sedimentation processes, J. Chem. Eng. 80 (2000) 105–117.